

\mathcal{C}^1 -HO – an implicit algorithm for validated enclosures of the solutions to variational equations for ODEs

Irmina Walawska and Daniel Wilczak

Faculty of Mathematics and Computer Science
Jagiellonian University
Łojasiewicza 6, 30-348 Kraków, Poland
{Irmina.Walawska, Daniel.Wilczak}@ii.uj.edu.pl

May 31, 2022

Abstract

We propose a new algorithm for computing validated bounds for the solutions to the first order variational equations associated to ODEs. The method uses a high order Taylor method as a predictor step and an implicit method based on the Hermite-Obreshkov interpolation as a corrector step. The proposed algorithm is an improvement of the \mathcal{C}^1 -Lohner algorithm by Zgliczyński and by its very construction cannot produce worse bounds.

As an application of the algorithm we give a computer assisted proof of the existence of an attractor in the Rössler system and we show that the attractor contains an invariant and uniformly hyperbolic subset on which the dynamics is chaotic, i.e. conjugated to the Bernoulli shift on two symbols.

AMS: 65G20, 65L05.

Keywords: validated numerics, initial value problem, variational equations, uniform hyperbolicity, chaos

1 Introduction.

The aim of this paper is to provide an algorithm that computes validated enclosures for the solutions to the following set of initial value problems

$$\begin{cases} \dot{x}(t) &= f(x(t)), \\ \dot{V}(t) &= Df(x(t)) \cdot V(t), \\ x(0) &\in [x_0], \\ V(0) &\in [V_0], \end{cases} \quad (1)$$

where $f : \mathbb{R}^n \rightarrow \mathbb{R}^n$ is a smooth function (usually analytic in the domain) and $[x_0] \subset \mathbb{R}^n$, $[V_0] \subset \mathbb{R}^{n^2}$ are sets of initial conditions. In contrast to standard numerical methods, one step of a validated algorithm for (1) produces sets $[x_1]$ and $[V_1]$ that guarantee to contain $x(h) \in [x_1]$ and $V(h) \in [V_1]$ for all initial conditions $x(0) \in [x_0]$ and $V(0) \in [V_0]$, where $h > 0$ is a time step (usually variable) of the method. The computations are performed in interval arithmetics [23] in order to obtain guaranteed bounds on the expressions we evaluate.

The equation for $V(t)$ is called the variational equation associated to an ODE. Solutions $V(t)$ give us an information about sensitivities of trajectories with respect to initial condition. They proved to be useful in finding periodic solutions, proving their existence and analysis of their stability [2, 3, 12, 13, 17, 19]. They are used to estimate invariant manifolds of periodic orbits [6, 7]. Derivatives with respect to initial conditions are used to prove the existence of connecting orbits [35, 4, 39] or even (non)uniformly hyperbolic and chaotic attractors [36, 38]. First and higher order derivatives with respect to initial conditions can be used to study some bifurcation problems [20, 39, 40]. This wide spectrum of applications is our main motivation for developing an efficient algorithm that produces sharp bounds on the solutions to (1).

In principle the problem (1) can be solved by any algorithm capable to compute validated solution to IVP for ODEs. There are several available algorithms and their implementations – just to mention few of them VNODE-LP [31, 32, 33, 37], COSY Infinity [5, 10, 8], CAPD [11], Valencia-IVP [29]. The above mentioned ODE solvers are internally higher order methods with respect to the initial state which means, that they use at least partial information about the derivatives with respect to initial condition to reduce *wrapping effect*. Therefore direct application of these solvers tends to higher effective dimension that the dimension of the phase space. In the case of VNODE-LP and CAPD it is $(n(n+1))^2$ which dramatically decreases performance of these methods when applied directly to the extended system (1). This key observation motivated developing the \mathcal{C}^1 -Lohner algorithm [43] which takes into account the block structure of (1) and works in n^2 effective dimension. Even in low dimensions it is orders of magnitude faster than direct application of a \mathcal{C}^0 solver to variational equations. On the other hand, it does not use derivatives of $V(t)$ with respect to other coefficients of V (i.e. second order derivatives of the original system) to better control the wrapping effect. This is why it usually produces worse estimations.

In this paper we propose an alternative \mathcal{C}^1 -HO algorithm for computation of validated solutions to (1). Our algorithm consists of two steps. First, the high order Taylor method is used as a predictor step. Then an implicit method based on the Hermite-Obreshkov formula is used to compute tighter bounds for the variational equations. The last step is motivated by the very famous and efficient algorithm proposed by Nedialkov and Jackson [31] and implemented by Nedialkov as the VNODE-LP package [37].

Our algorithm, by its very construction, cannot produce worse estimations than the \mathcal{C}^1 -Lohner algorithm. Complexity analysis (see Section 3) shows that

in low dimensions it is slower than \mathcal{C}^1 -Lohner algorithm by the factor 9/8, only. On the other hand, this lack of performance is compensated by a significantly smaller truncation error of the method. This allows to make larger time steps when computing the trajectories and thus our algorithm appears to be slightly faster than the \mathcal{C}^1 -Lohner in real applications – see Section 5, for the case study.

We would like to emphasize that the proposed method can be directly extended to the nonautonomous case without increasing the effective dimension of the problem. We omit, however, this case to do not cloud the main ideas of the algorithm by technicalities and more complicated notation. We provide an implementation of the \mathcal{C}^1 -HO algorithm [11] for nonautonomous case, as well.

As an application of the proposed algorithm we give a computer assisted proof of the following new result concerning the Rössler system [30].

Theorem 1 *For the parameter values $a = 5.7$ and $b = 0.2$ the system*

$$\begin{cases} \dot{x} &= -y - z \\ \dot{y} &= x + by \\ \dot{z} &= b + z(x - a) \end{cases} \quad (2)$$

admits a compact, connected invariant set \mathcal{A} called an attractor. There is an invariant subset $\mathcal{H} \subset \mathcal{A}$ on which the dynamics is chaotic and uniformly hyperbolic.

The paper is organized as follows. In Section 1.1 we introduce symbols and notations used in the paper. Section 2 contains description of the algorithm and proof of its correctness. In Section 3 we analyze complexity of the \mathcal{C}^1 -HO algorithm and compare it to the complexity of the \mathcal{C}^1 -Lohner algorithm. In Section 4 we compare bounds obtained from \mathcal{C}^1 -Lohner and \mathcal{C}^1 -HO algorithms on several examples. In Section 5 we give a more detailed statement and proof of Theorem 1 – see Theorem 4. We will also discuss how the time of computation depends on the choice of \mathcal{C}^1 -Lohner and \mathcal{C}^1 -HO algorithms to integrate variational equations.

1.1 Notation.

By Id we will denote the identity matrix of the dimension clear from the context. By Df we will denote derivative of a smooth function $f : \mathbb{R}^n \rightarrow \mathbb{R}^m$. By $D_x f$ we will denote the partial derivative of f with respect to x .

The local flow induced by an ordinary differential equation (ODE) $\dot{x}(t) = f(x(t))$ will be denoted by φ , i.e. $\varphi(\cdot, x) = x(\cdot)$ is the unique solution passing through x at the time zero. We will often identify an element $x \in \mathbb{R}^n$ with the function $x(\cdot) = \varphi(\cdot, x)$. Put $\psi(t, x, V) = D_x \varphi(t, x) \cdot V$. Clearly $\psi(\cdot, x, V)$ is a solution to the first order variational equation associated to an ODE with the initial conditions x and V .

Let $f : \mathbb{R} \rightarrow \mathbb{R}^n$ be a smooth function. By $f^{(i)}(x)$ we denote the vector of i -th derivatives of f . Normalized derivatives (Taylor coefficients) will be

denoted by $f^{[i]}(x) = \frac{1}{i!} f^{(i)}(x)$. We will apply this notation of derivatives and Taylor coefficients of the flows φ and ψ taken with respect to the time variable

$$\begin{aligned}\varphi^{[i]}(t, x) &:= (\varphi^{[i]}(\cdot, x))(t), \\ \psi^{[i]}(t, x, V) &:= (\psi^{[i]}(\cdot, x, V))(t).\end{aligned}$$

Interval objects will be always denoted in square brackets, for instance $[a] = [\underline{a}, \bar{a}]$ is an interval and $[v] = ([v_1], \dots, [v_n])$ is an interval vector. Matrices or interval matrices will be denoted by capital letters, for example $[A]$. Vectors and scalars will be always denoted by small letters. We will also identify Cartesian product of intervals $[v_1] \times \dots \times [v_n]$ with a vector of intervals $([v_1], \dots, [v_n])$ thus interval vectors can be seen as subsets of \mathbb{R}^n . The same identification will apply to interval matrices.

The midpoint of an interval $[a] = [\underline{a}, \bar{a}]$ will be denoted by $\hat{a} = \frac{1}{2}(\underline{a} + \bar{a})$. The same convention will be used to denote midpoint of an interval vector or an interval matrix; for example for $[v] = ([v_1], \dots, [v_n])$ we put $\hat{v} = (\hat{v}_1, \dots, \hat{v}_n)$. Sometimes, we will denote the midpoint of products of interval objects by $\text{mid}([V][r])$.

Through this paper interval vectors or interval matrices marked with tilde $[\tilde{y}]$, $[\tilde{V}]$ will always refer to rough enclosures for the solutions to IVP problem (1) – see Section 2.1 for details.

2 The algorithm.

Consider the initial value problem (1) and assume that we have already proved the existence of the solutions at time t_k and we have computed rigorous bounds $[x_k]$ and $[V_k]$ for $\varphi(t_k, [x_0]) \subset [x_k]$, $\psi(t_k, [x_0], [V_0]) \subset [V_k]$, respectively. Let us fix a time step $h_k > 0$. A rigorous numerical method for (1) consist usually of the following two steps:

- computation of a rough enclosure. In this step the algorithm validates that solutions indeed exist over the time interval $[t_k, t_k + h_k]$ and it produces sets $[\tilde{y}]$ and $[\tilde{V}]$, called rough enclosures, which satisfy

$$\varphi([0, h_k], [x_k]) \subset [\tilde{y}], \quad (3)$$

$$\psi([0, h_k], [x_k], \text{Id}) \subset [\tilde{V}]. \quad (4)$$

- computation of possible tight bounds $[x_{k+1}]$, $[V_{k+1}]$ satisfying $\varphi(t_k + h_k, [x_0]) \subset [x_{k+1}]$ and $\psi(t_k + h_k, [x_0], [V_0]) \subset [V_{k+1}]$.

In the sequel we will give details of each part of the proposed algorithm.

2.1 Computation of a rough enclosure.

This section is devoted to describe a method for finding rough enclosures (3-4). The key observation is that the equation for V in (1) is linear in V which implies that the following identity holds true

$$\psi(t_k + h_k, x_0, V_0) = \psi(h_k, \varphi(t_k, x_0), \text{Id}) \cdot \psi(t_k, x_0, V_0)$$

provided all quantities are well defined. This implies that

$$\psi(t_k + h_k, [x_0], [V_0]) \subset \psi(h_k, [x_k], \text{Id}) \cdot [V_k]. \quad (5)$$

Hence, it is enough to use Id as an initial condition for the variational equations when computing a rough enclosure $[\tilde{V}]$.

One approach to find rough enclosures $[\tilde{y}]$ and $[\tilde{V}]$ is to compute them separately. Given a set $[\tilde{y}]$ satisfying (3) and computed by any algorithm we can try to find an interval matrix $[\tilde{V}]$ such that

$$\text{Id} + [0, h_k] Df([\tilde{y}]) \cdot [\tilde{V}] \subset [\tilde{V}]. \quad (6)$$

If we succeed then the interval matrix $[\tilde{V}]$ satisfies (4). This method is known as the First Order Enclosure (FOE). It has, however, at least one significant disadvantage. If we already know that the solutions to the main equations exist over the time step h_k ($[\tilde{y}]$ has been computed) there is no reason to shorten this time step because solutions to variational equation also exist over the same time range. However, this shortening might be necessary to fulfill the condition (6). To avoid this drawback Zgliczyński proposes [43] a method based on logarithmic norms that always computes an enclosure $[\tilde{V}]$ satisfying (4) for the same time step h_k provided we were able to find an enclosure $[\tilde{y}]$ satisfying (3). This type of enclosure is also used in the C^r -Lohner algorithm [41] for higher order variational equations.

Another strategy is to use the High Order Enclosure (HOE) [9, 33, 32]. The authors propose to predict a rough enclosure of the form

$$[\tilde{y}] = \sum_{i=0}^m [0, h_k]^i \varphi^{[i]}(0, [x_k]) + [\varepsilon], \quad (7)$$

where $[\varepsilon]$ is an interval vector centered at zero. The inclusion

$$[0, h_k]^{m+1} \varphi^{[m+1]}(0, [\tilde{y}]) \subset [\varepsilon] \quad (8)$$

implies that the set $[\tilde{y}]$ is indeed a rough enclosure, i.e. it satisfies (3). If the inclusion (8) is not satisfied then we can always find $\bar{h}_k < h_k$ such that (8) holds true with this time step and thus $[\tilde{y}]$ is a rough enclosure for the time step \bar{h}_k . This strategy is very efficient because we do not need to recompute $[\tilde{y}]$. Furthermore, with quite high order m and a reasonable algorithm for time step prediction, we usually have $\bar{h}_k/h_k = \left(\frac{\|\varepsilon\|}{\|\varphi^{[m+1]}(0, [\tilde{y}])\|} \right)^{1/(m+1)} \approx 1$.

The above method can be used to find simultaneously two enclosures $([\tilde{y}], [\tilde{V}])$ for the entire system (1). We predict $[\tilde{y}]$ as in (7) and

$$[\tilde{V}] = \sum_{i=0}^m [0, h_k]^i \psi^{[i]}(0, [x_k], \text{Id}) + [E]. \quad (9)$$

Then we check simultaneously (8) and

$$[0, h_k]^{m+1} \psi^{[m+1]}(0, [\tilde{y}], \text{Id}) [\tilde{V}] \subset [E]. \quad (10)$$

Algorithm 1: Predictor.

Data: m - natural number (order of the Taylor method)
Data: h_k - positive real number (current time step)
Data: $[x_k], [\tilde{y}]$ - interval vectors
Data: $[\tilde{V}]$ - interval matrix
Result: $([x_{k+1}^0], [r^0], [V^0], [R^0]) \subset \mathbb{R}^n \times \mathbb{R}^n \times \mathbb{R}^{n^2} \times \mathbb{R}^{n^2}$
begin
 $[A] \leftarrow \sum_{i=0}^m h_k^i \psi^{[i]}(0, [x_k], \text{Id});$
 $[\tilde{y}] \leftarrow \sum_{i=0}^m h_k^i \varphi^{[i]}(0, \hat{x}_k);$
 $[y] \leftarrow \sum_{i=0}^m h_k^i \varphi^{[i]}(0, [x_k]);$
 $[r^0] \leftarrow [0, h_k]^{m+1} \varphi^{[m+1]}(0, [\tilde{y}]);$
 $[x_{k+1}^0] \leftarrow ([\tilde{y}] + [A]([x_k] - \hat{x}_k)) \cap [y] + [r^0];$
 $[R^0] \leftarrow [0, h_k]^{m+1} \psi^{[m+1]}(0, [\tilde{y}], \text{Id})[\tilde{V}];$
 $[V^0] \leftarrow [A] + [R^0];$
 return $([x_{k+1}^0], [r^0], [V^0], [R^0]);$

Due to linearity of the equation for variational equations we can consider two strategies when (10) is not satisfied. We can

1. either shorten the time step as we do in (8),
2. or compute $[\tilde{V}^0]$ from the logarithmic norms for the same time step h_k as proposed in [43], set $[E] = [0, h_k]^{m+1} \psi^{[m+1]}(0, [\tilde{y}], \text{Id})[\tilde{V}^0]$. Then $[\tilde{V}]$ computed as in (9) with such $[E]$ satisfies (4).

Note that in both cases we do not need to recompute the coefficients $\psi^{[i]}(0, [\tilde{y}], \text{Id})$ which is very expensive. The first strategy is recommended when the tolerance per one step is specified which means that there is a maximal norm of $[E]$ which should not be exceeded. The second strategy applies when the fixed time step is used (by the user choice or application specific reason).

Our tests show that \mathcal{C}^1 version of (HOE) gives better results than the approach proposed by Zgliczyński which uses logarithmic norms. Since computing a rough enclosure (4) is not the main topic of the paper we omit details here.

In what follows we assume that we have an abstract routine (an oracle) that returns three quantities: $h_k, [\tilde{y}], [\tilde{V}]$ for which the properties (3) and (4) hold true.

2.2 The predictor step.

We give a short description of the \mathcal{C}^1 -Lohner algorithm [43] which will be used as a predictor step in the \mathcal{C}^1 -HO algorithm.

Lemma 2 *Assume $h_k, [x_k], [\tilde{y}], [\tilde{V}]$ are such that (3) and (4) hold true. Then*

the quantities $([x_{k+1}^0], [r^0], [V^0], [R^0])$ computed by the Algorithm 1 satisfy

$$\varphi(h_k, [x_k]) \subset [x_{k+1}^0], \quad (11)$$

$$\psi(h_k, [x_k], \text{Id}) \subset [V^0], \quad (12)$$

$$[0, h_k]^{m+1} \varphi^{[m+1]}(0, [\tilde{y}]) \subset [r^0], \quad (13)$$

$$[0, h_k]^{m+1} \psi^{[m+1]}(0, [\tilde{y}], [\tilde{V}]) \subset [R^0]. \quad (14)$$

Proof: The Taylor theorem with Lagrange remainder implies that for $x_k \in [x_k]$ and each component $j = 1, \dots, n$ there holds

$$\varphi_j(h_k, x_k) = \sum_{i=0}^m h_k^i \varphi_j^{[i]}(0, x_k) + h_k^{m+1} \varphi_j^{[m+1]}(\tau_j, x_k) \quad (15)$$

for some $\tau_j \in (0, h_k)$. By the assumptions $\varphi(\tau_j, x_k) \in [\tilde{y}]$ and by the group property of the flow we have

$$\varphi_j^{[m+1]}(\tau_j, x_k) = \varphi_j^{[m+1]}(0, \varphi(\tau_j, x_k)) \in \varphi_j^{[m+1]}(0, [\tilde{y}]).$$

Therefore

$$\varphi(h_k, x_k) \in \sum_{i=0}^m h_k^i \varphi_j^{[i]}(0, x_k) + h_k^{m+1} \varphi^{[m+1]}(0, [\tilde{y}]) \subset [y] + [r^0].$$

Since $[x_k]$ is convex, we can apply the mean value form to the polynomial part of (15) and we obtain

$$\sum_{i=0}^m h_k^i \varphi^{[i]}(0, x_k) \in \sum_{i=0}^m h_k^i \varphi^{[i]}(0, \hat{x}_k) + [A](x_k - \hat{x}_k) \subset [\tilde{y}] + [A]([x_k] - \hat{x}_k).$$

Gathering this together we get

$$\varphi(h_k, [x_k]) \subset ([\tilde{y}] + [A]([x_k] - \hat{x}_k)) \cap [y] + [r^0] = [x_{k+1}^0]. \quad (16)$$

In a similar way we deduce that for $x_k \in [x_k]$ and for each component $j, c = 1, \dots, n$ there holds

$$\psi_{j,c}^{[m+1]}(\tau_{j,c}, x_k, \text{Id}) \in \psi_{j,c}^{[m+1]}(0, [\tilde{y}], [\tilde{V}])$$

for $j, c = 1, \dots, n$ and in consequence

$$\psi(h_k, [x_k], \text{Id}) \subset [A] + [R^0] = [V^0].$$

■

2.3 The corrector step.

The goal of this section is to set forth a one-step method which refines results obtained from the predictor step and returns tighter rigorous bounds for the solution to ODE and to associated variational equation (1). The method combines the algorithm by Nedialkov and Jackson [31] based on the Hermite-Obreshkov interpolation formula with the C^1 -Lohner algorithm for variational equations proposed by Zgliczyński [43]. For the self-consistency of the article we recall here the key ideas of the Hermite-Obreshkov method.

For natural numbers p, q, i such that $i \leq q$ we put

$$c_i^{q,p} = \binom{q}{i} / \binom{p+q}{i}.$$

For a smooth function $u : \mathbb{R} \rightarrow \mathbb{R}^n$ and real numbers h, t we define

$$\Psi_{q,p}(h, u, t) = \sum_{i=0}^q c_i^{q,p} h^i u^{[i]}(t).$$

Using this notation the Hermite-Obreshkov [26] formula reads

$$\Psi_{q,p}(-h, u, h) = \Psi_{p,q}(h, u, 0) + (-1)^q c_q^{q,p} h^{p+q+1} R(h, u) \quad (17)$$

where

$$R(h, u) = \left(u^{[p+q+1]}(\tau_1), \dots, u^{[p+q+1]}(\tau_n) \right), \quad \tau_i \in (0, h), i = 1, \dots, n.$$

The key observation which was the main motivation to develop rigorous numerical method based on this formula is that the coefficient $c_q^{q,p} = \binom{p+q}{q}^{-1}$ can be very small for $p = q$ not too small. Thus this formula can have significantly smaller remainder than the Lagrange remainder used in the Taylor series method.

Now we would like to apply (17) to the flows φ and $\psi := D_x \varphi$. Let $[x_k]$ be a set of initial conditions and assume that from the predictor step we have computed $([x_{k+1}^0], [r^0], [V^0], [R^0])$ satisfying (11–14).

Let us fix positive integers p, q such that $m = p + q$, $x_k \in [x_k]$ and put $x_{k+1} = \varphi(h, x_k)$. The formula (17) applied to this case reads

$$\sum_{i=0}^q c_i^{q,p} (-h_k)^i \varphi^{[i]}(0, x_{k+1}) = \sum_{i=0}^p c_i^{p,q} h_k^i \varphi^{[i]}(0, x_k) + \varepsilon,$$

where $\varepsilon \in (-1)^q c_q^{q,p} [r^0]$. Identifying vectors x_k, x_{k+1} with unique solutions $x_k(\cdot), x_{k+1}(\cdot)$ to the ODE passing through them at time zero we obtain equivalent but shorter form

$$\Psi_{q,p}(-h_k, x_{k+1}, 0) = \Psi_{p,q}(h_k, x_k, 0) + \varepsilon. \quad (18)$$

Take the midpoints $\hat{x}_{k+1}^0 \in [x_{k+1}^0]$, $\hat{x}_k \in [x_k]$. Since interval vectors are convex sets and the local flow is a smooth function in both variables we can apply the mean-value form to both sides of (18) and we get

$$\Psi_{q,p}(-h_k, \hat{x}_{k+1}^0, 0) + J_-(x_{k+1} - \hat{x}_{k+1}^0) = \Psi_{p,q}(h_k, \hat{x}_k, 0) + J_+(x_k - \hat{x}_k) + \varepsilon$$

for some

$$\begin{aligned} J_- &\in [D_x \Psi_{q,p}(-h_k, [x_{k+1}^0], 0)], \\ J_+ &\in [D_x \Psi_{p,q}(h_k, [x_k], 0)]. \end{aligned}$$

We obtained a linear equation for x_{k+1}

$$J_-(x_{k+1} - \hat{x}_{k+1}^0) = J_+(x_k - \hat{x}_k) + (\Psi_{p,q}(h_k, \hat{x}_k, 0) - \Psi_{q,p}(-h_k, \hat{x}_{k+1}^0, 0)) + \varepsilon \quad (19)$$

in which the matrices J_{\pm} are unknown but they can be rigorously bounded. Denoting

$$\begin{aligned} [\delta] &= \Psi_{p,q}(h_k, \hat{x}_k, 0) - \Psi_{q,p}(-h_k, \hat{x}_{k+1}^0, 0), \\ [\varepsilon] &= (-1)^q c_q^{q,p} [r^0], \\ [J_-] &= [D_x \Psi_{q,p}(-h_k, [x_{k+1}^0], 0)], \\ [J_+] &= [D_x \Psi_{p,q}(h_k, [x_k], 0)], \\ [S] &= \text{Id} - \hat{J}_-^{-1} [J_-], \\ [r] &= \hat{J}_-^{-1} ([\delta] + [\varepsilon]) + [S]([x_{k+1}^0] - \hat{x}_{k+1}^0) \end{aligned}$$

and applying the interval Krawczyk operator [16, 25, 1] to the linear system (19) we obtain that for $x_k \in [x_k]$ there holds

$$\varphi(h_k, x_k) = x_{k+1} \in \hat{x}_{k+1}^0 + \left(\hat{J}_-^{-1} [J_+] \right) ([x_k] - \hat{x}_k) + [r] \quad (20)$$

which is the main evaluation formula in the interval Hermite-Obreshkov method for IVPs presented in [31]. Note that this formula has exactly the same structure as (16) used in the predictor step.

The interval matrix $[S]$ contains zero and its diameter tends to zero with h_k approaching zero. The vector $[\delta]$ is almost a point vector and $[\varepsilon]$ we can make as small as we need (manipulating the time step h_k). Therefore the total error accumulated in $[r]$ is usually very thin in comparison to the size of the set $[x_k]$ we propagate. Thus the main source of overestimation when evaluating (20) comes from the propagation of the product $\left(\hat{J}_-^{-1} [J_+] \right) ([x_k] - \hat{x}_k)$. There is a wide literature on how to reduce this wrapping effect for such propagation (see [24] for a survey) and we will give some details concerning this issue in Section 2.4.

In what follows we argue that with a little additional cost we can compute possible tighter enclosure for the solutions to variational equations than the bound $[V^0]$ obtained from the predictor step. Let us fix $x_k \in [x_k]$ and put

$V = \psi(h_k, x_k, \text{Id})$. Applying (17) to the solutions to variational equations we obtain

$$\sum_{i=0}^q c_i^{q,p} (-h_k)^i \psi^{[i]}(0, x_{k+1}, V) = \sum_{i=0}^p c_i^{p,q} h_k^i \psi^{[i]}(0, x_k, \text{Id}) + E,$$

where $E \in (-1)^q c_q^{q,p} [R^0]$. Since ψ is linear in V , we obtain that the matrix $V = \psi(h_k, x_k, \text{Id})$ belongs to the solution set to the linear equation

$$[J_-]V = [J_+] + [E],$$

where $[E] = (-1)^q c_q^{q,p} [R^0]$. Note that from the predictor step we already know that $V \in [V^0]$. Applying the interval Krawczyk operator [16] to this linear system we obtain

$$V \in \hat{J}_-^{-1}([J_+] + [E]) + (\text{Id} - \hat{J}_-^{-1}[J_-])[V^0] = \hat{J}_-^{-1}([J_+] + [E]) + [S][V^0].$$

Due to linearity of equation for variational equations we can reuse the matrices $[J_-]$, $[J_+]$, $[S]$ and \hat{J}_-^{-1} computed in the corrector step for φ . Thus the additional cost is just few matrix additions and multiplications. Algorithm 2 and Lemma 3 summarize the above considerations.

Algorithm 2: Corrector.

Data: p, q - positive integers
Data: h_k - positive real number
Data: $[x_k]$ - interval vectors
Data: $([x_{k+1}^0], [r^0], [V^0], [R^0])$ - from the predictor step with $m = p + q$
Result: $([x_{k+1}], [V])$
begin

$[\delta] \leftarrow \Psi_{p,q}(h_k, \hat{x}_k, 0) - \Psi_{q,p}(-h_k, \hat{x}_{k+1}^0, 0);$
$[\varepsilon] \leftarrow (-1)^q c_q^{q,p} [r^0];$
$[J_-] \leftarrow [D_x \Psi_{q,p}(-h_k, [x_{k+1}^0], 0)];$
$[J_+] \leftarrow [D_x \Psi_{p,q}(h_k, [x_k], 0)];$
$[S] \leftarrow \text{Id} - \hat{J}_-^{-1}[J_-];$
$[r] \leftarrow \hat{J}_-^{-1}([\delta] + [\varepsilon]) + [S]([x_{k+1}^0] - \hat{x}_{k+1}^0);$
$[R] \leftarrow \hat{J}_-^{-1}([J_+] + (-1)^q c_q^{q,p} [R^0]);$
$[x_{k+1}] \leftarrow \left(\hat{x}_{k+1}^0 + \left(\hat{J}_-^{-1}[J_+] \right) ([x_k] - \hat{x}_k) + [r] \right) \cap [x_{k+1}^0];$
$[V] \leftarrow ([R] + [S][V^0]) \cap [V^0];$
return $([x_{k+1}], [V]);$

Lemma 3 Assume $h_k, [x_k], [\tilde{y}], [\tilde{V}]$ are such that (3) and (4) hold true and the quadruple $([x_{k+1}^0], [r^0], [V^0], [R^0])$ is returned by the predictor step (Algorithm 1). Then the quantities $([x_{k+1}], [V])$ computed by the Algorithm 2 satisfy

$$\varphi(h_k, [x_k]) \subset [x_{k+1}], \quad (21)$$

$$\psi(h_k, [x_k], \text{Id}) \subset [V]. \quad (22)$$

We would like to emphasize that by its construction the proposed algorithm always returns tighter bounds than the \mathcal{C}^1 -Lohner algorithm because the result obtained from the corrector step is intersected with the bound obtained from the predictor step.

2.4 Propagation of product of interval objects.

It is well known that evaluation of expressions in interval arithmetics can produce large overestimation due to dependency of variables and the wrapping effect [23, 1, 25, 22]. In order to reduce this undesirable drawback we follow the ideas from [22, 24, 43, 31] and we will represent subsets of \mathbb{R}^n and \mathbb{R}^{n^2} in the forms (doubletons in [24] terminology)

$$[x_k] = x_k + C_k[r_k] + B_k[s_k], \quad (23)$$

$$[V_k] = V_k + A_k[R_k] + Q_k[S_k]. \quad (24)$$

The initial conditions $([x_0], [V_0])$ of (1) are assumed to be already in the form (23–24). The parallelepipeds $x_k + C_k[r_k]$ and $V_k + A_k[R_k]$ are used to store the main part of the sets $[x_k]$ and $[V_k]$, respectively. The terms $B_k[s_k]$ and $Q_k[S_k]$ are used to collect all usually thin quantities that appear during the computation.

According to (5) the bound for $\psi(t_k + h_k, [x_0], [V_0])$ can be computed as

$$[V_{k+1}] = [V][V_k].$$

Substituting the representation (24) we obtain

$$[V_{k+1}] \subset [V] (V_k + A_k[R_k] + Q_k[S_k]) \cap (V_{k+1} + A_{k+1}[R_{k+1}] + Q_{k+1}[S_{k+1}]),$$

where the new representation is computed as follows

$$\begin{aligned} [\Delta A] &= ([V] - \hat{V}) (V_k + A_k[R_k]), \\ V_{k+1} &= \hat{V}V_k \\ A_{k+1} &= \hat{V}A_k, \\ [S_{k+1}] &= (Q_{k+1}^{-1}[V][Q_k]) [S_k] + Q_{k+1}^{-1}[\Delta A], \\ [R_{k+1}] &= [R_k]. \end{aligned}$$

In principle, the matrix Q_{k+1} can be chosen as any invertible matrix. The numerical experiments [22, 24, 31, 43] show that one of the most efficient strategies in reducing the wrapping effect is to compute Q_{k+1} as an orthogonal matrix from the QR decomposition of the point matrix $\hat{V}Q_k$. Note, that the even if the matrix Q_{k+1} is a point matrix the inverse Q_{k+1}^{-1} must be computed rigorously in interval arithmetics.

Similar strategy is used for propagation of products in

$$\begin{aligned} [x_{k+1}] &\subset \hat{x}_{k+1}^0 + \left(\hat{J}_-^{-1}[J_+] \right) ([x_k] - \hat{x}_k) + [r] \\ &= \hat{x}_{k+1}^0 + \left(\hat{J}_-^{-1}[J_+] \right) (C_k[r_k] + B_k[s_k]) + [r] \end{aligned}$$

– consult [22, 24, 31, 43] for details.

3 Complexity.

In this section we explain why the \mathcal{C}^1 -HO algorithm may perform better than the \mathcal{C}^1 -Lohner algorithm, even if it has higher computational complexity. Large numerical and theoretical study was made to compare the Interval Hermite-Obreshkov method (IHO) with the Interval Taylor Series Method (ITS) [32]. It has been shown that, with the same step size and order, the IHO method is more stable and produces smaller enclosures than the ITS method on constant coefficient problems. Furthermore, the IHO method allows usually for much larger stepsize than the ITS method, thus saving computation time during the whole integration. However, comparison this two methods in the nonlinear case is not as simple as in the constant coefficient case. Our goal is to predict the benefits of performing additional calculations required by the IHO method applied to (1).

3.1 Cost of \mathcal{C}^1 -Lohner and \mathcal{C}^1 -HO methods per one step.

We assume that both predictor (Algorithm 1) and corrector (Algorithm 2) have the same order, that is, if the order of the predictor is m , we consider the corrector step with p and q such that $m = p + q$. In what follows we will list the most time-consuming items of the predictor and corrector which are the core of their computational complexity.

Let us denote by c_f the cost of the evaluation of the vector field (1). For the \mathcal{C}^1 -Lohner step we need the following operations (predictor step and propagation of doubleton representations)

- simultaneous computation of $\varphi^{[i]}(0, [x_k])$ and $\psi^{[i]}(0, [x_k], \text{Id})$ up to order m . This is performed by means of the automatic differentiation and it takes $\frac{1}{2}c_f(2n+1)(m+1)(m+2)$ operations – see [14],
- simultaneous computation of $\varphi^{[i]}(0, [\tilde{y}])$ and $\psi^{[i]}(0, [\tilde{y}], \text{Id})$ up to order $m+1$. This is performed by means of the automatic differentiation and it takes $\frac{1}{2}c_f(2n+1)(m+2)(m+3)$ operations – see [14],
- 13 matrix by matrix multiplications, 2 point matrix inversions and 2 point matrix QR decompositions. Approximate QR decomposition of a point matrix is much cheaper than the product of interval matrices and we may assume that it takes at most n^3 . The inversion of a point matrix which is very close to orthogonal is performed by means of the interval Krawczyk operator [16] and takes n^3 (one multiplication) because an approximate result is already known (transposition of an approximate orthogonal matrix). Thus, the total cost of all matrix operations listed above is at most $17n^3$.

We did not list cheaper operations like additions, intersections of interval objects, matrix by vector products and polynomial evaluations.

To sum up, the total costs of the \mathcal{C}^1 -Lohner step is

$$C_{LO}(n, m) = c_f(2n + 1)(m + 2)^2 + 17n^3.$$

In the \mathcal{C}^1 -HO method we can reuse the Taylor coefficients of φ and ψ computed in predictor step which are needed for computation of $[J_+]$ matrix and $\Psi_{p,q}(h_k, \hat{x}_k, 0)$. Thus additional cost is

- computation of $\psi^{[i]}(0, [x_{k+1}^0], \text{Id})$ up to order q . This is performed by means of the automatic differentiation and it takes $\frac{1}{2}c_f(2n+1)(q+1)(q+2)$ operations – see [14],
- computation of $\Psi_{q,p}(-h_k, \hat{x}_{k+1}^0, 0)$ takes $\frac{1}{2}c_f(q+1)(q+2)$,
- inversion of the point matrix \hat{J}_- takes at most $2n^3$ and 4 matrix multiplications require $4n^3$ operations.

The total additional cost of the \mathcal{C}^1 -HO step is

$$c_f(n + 1)(q + 1)(q + 2) + 6n^3.$$

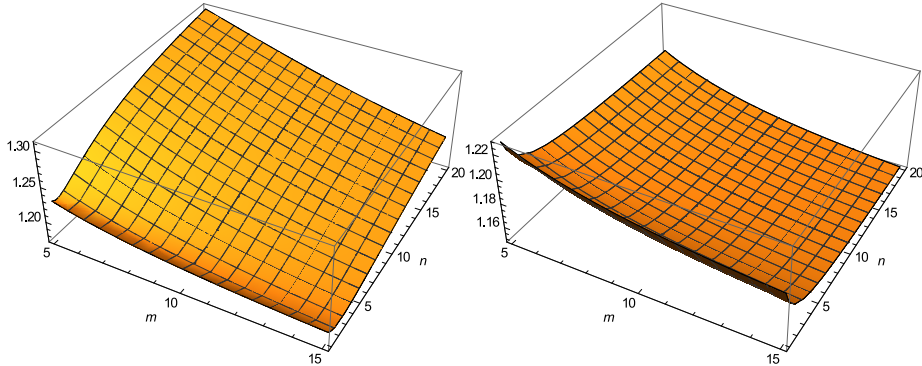


Figure 1: Plot of $C_{HO}(n, m)/C_{LO}(n, m)$ for $c_f = n$ and $c_f = n^2$, respectively.

Assume that m is an even number and take $q = p = \frac{m}{2}$. Then the above additional cost of the \mathcal{C}^1 -HO method reads

$$\frac{1}{4}c_f(n + 1)(m + 2)(m + 4) + 6n^3.$$

Hence, total computational complexity of the \mathcal{C}^1 -HO method is

$$C_{HO}(n, m) = C_{LO}(n, m) + \frac{1}{4}c_f(n+1)(m+2)(m+4) + 6n^3.$$

In general the complexity depends on the cost of the vector field evaluation c_f which can be arbitrary. In Fig. 1 we plot the graph of C_{HO}/C_{LO} for two cases. The case $c_f = n$ means that the number of nonlinear terms in the vector field is equal to the dimension of the problem. We observe that if order m of the method is much smaller than the dimension n then the complexity is dominated by the matrix operations and we have

$$\lim_{n \rightarrow \infty} C_{HO}(n, m)/C_{LO}(n, m) = \frac{23}{17} \approx 1.35294.$$

for all fixed values of m . We observe, however, that for reasonable dimensions and orders this factor is much smaller than the limit value.

A model example for the $c_f = n^2$ case is a second order polynomial vector field with nonzero coefficients in the quadratic terms. In this case we have

$$\lim_{n \rightarrow \infty} C_{HO}(n, m)/C_{LO}(n, m) = \frac{9m^2 + 38m + 132}{8m^2 + 3m + 100}.$$

The above analysis shows that the additional cost of the \mathcal{C}^1 -HO method in a typical nonlinear case approaches 1/8. In the next section we will argue that this extra cost of the \mathcal{C}^1 -HO method is compensated by the larger time steps this method can perform without losing the accuracy.

3.2 Maximal allowed time step for a fixed error tolerance.

To get whole insight in compared methods we ask the following question: given an acceptable tolerance ε per one step what is the maximal time step h of both methods that guarantees achieving this constraint. For the \mathcal{C}^1 -Lohner method we have to solve the following inequality

$$\left\| h^{m+1} \varphi^{[m+1]}(0, [\tilde{y}]) \right\| \leq \varepsilon.$$

In general it is very difficult to answer this question because $[\tilde{y}] = [\tilde{y}(h)]$ depends on h . If $[x_k]$ is a point and ε is very small we can assume that the vector field is almost constant near $[x_k]$ and thus $\varphi^{[m+1]}(0, [\tilde{y}]) \approx \varphi^{[m+1]}(0, [x_k])$. Since $[x_k] \subset [\tilde{y}]$ we always have $\|\varphi^{[m+1]}(0, [x_k])\| \leq \|\varphi^{[m+1]}(0, [\tilde{y}])\|$. With this simplification we obtain an upper bound for the time step

$$h_{LO} := h = \sqrt[m+1]{\frac{\varepsilon}{\|\varphi^{[m+1]}(0, [x_k])\|}}.$$

For the \mathcal{C}^1 -HO method we obtain the following upper bound for the time step

$$h_{HO} := h = \sqrt[m+1]{\binom{m}{\lceil \frac{m}{2} \rceil} \frac{\varepsilon}{\|\varphi^{[m+1]}(0, [x_k])\|}},$$

where by $\lceil m/2 \rceil$ we denote the smallest integer not smaller than $m/2$. Put

$$g(m) := h_{HO}/h_{LO} = \sqrt[m+1]{\binom{m}{\lceil \frac{m}{2} \rceil}}.$$

It is easy to show that

$$\lim_{m \rightarrow \infty} g(m) = 2.$$

In Fig. 2 we can observe that the values of $g(m)$ rapidly grow for small values of m . This is very important from the practical point of view - even for small order $m = 6$ the \mathcal{C}^1 -HO method allows up to 53% larger time steps than the \mathcal{C}^1 -Lohner method. For $m = 16$ this is 74%. For larger values of the tolerance ε the computed enclosure $[\tilde{y}]$ for $h = h_{LO}$ is usually significantly smaller than that computed for $h = h_{HO}$ which affects the norm $\|\varphi^{[m+1]}(0, [\tilde{y}])\|$. Therefore the value $g(m)$ is a theoretical upper bound for the possible growth ratio of the time step in the \mathcal{C}^1 -HO method achievable when $\varepsilon \rightarrow 0$.

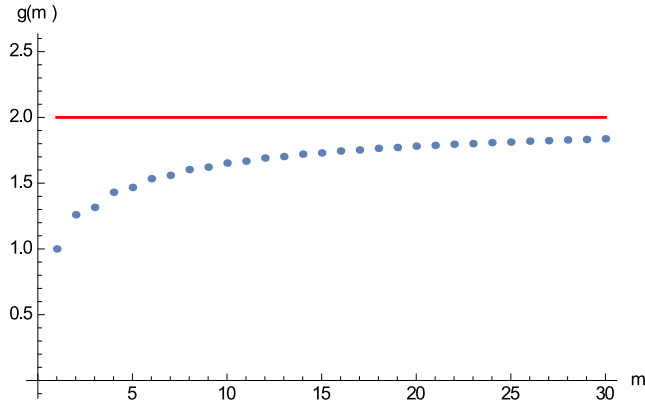


Figure 2: Plot of the theoretical maximal factor of maximal time step in the \mathcal{C}^1 -HO and \mathcal{C}^1 -Lohner methods for a fixed tolerance.

4 Benchmarks.

In this section we present the results of a comparison of the \mathcal{C}^1 -Lohner algorithm to the \mathcal{C}^1 -HO algorithm. The structure of tests is the following. For a given ODE

- we take an initial condition u which is an approximate periodic orbit for this system,
- we integrate the variational equations along this periodic orbit using the \mathcal{C}^1 -Lohner and \mathcal{C}^1 -HO algorithms with the same algorithm for rough enclosure (HOE), the same order $m = p + q$ of the methods and a constant time step $h_k = \text{const}$,

- we compare the logarithm of the maximal diameter of the interval matrix $[V_k]$ (diameter of the widest component) computed by means of the two algorithms,
- we repeat the above two steps six times: for two different orders of the numerical methods each for three different time steps.

Fixing the time steps allows us to compare size of enclosure returned by the two algorithms over the same time step. This will allow us to conclude that \mathcal{C}^1 -HO algorithm can perform bigger time steps than \mathcal{C}^1 -Lohner algorithm without significant lose of accuracy. The comparison of the two algorithms with variable time steps will be given in Section 5.

The above test is performed for four ODEs: the Lorenz [21] system, the Hénon-Heiles system [15], the Planar Restricted Three Body Problem (PCR3BP) and a 10-dimensional moderate stiff ODE. Below we give initial conditions and discuss obtained results.

The Lorenz system [21] for “classical” parameters is given by

$$\begin{cases} \dot{x} &= 10(y - x), \\ \dot{y} &= x(28 - z) - y, \\ \dot{z} &= xy - \frac{8}{3}z. \end{cases} \quad (25)$$

The Hénon-Heiles system [15] is a hamiltonian ODE given by

$$\begin{cases} \ddot{x} &= -x(1 + 2y), \\ \ddot{y} &= x^2 - y(1 + y). \end{cases} \quad (26)$$

The PCR3BP is a mathematical model that describes motion of a small body with negligible mass in the gravitational influence of two big bodies. The motion is restricted to the plane and the two main primaries rotate around their common mass centre. The equations for motion of the small body is then given by

$$\begin{cases} \ddot{x} - 2\dot{y} = D_x\Omega(x, y), \\ \ddot{y} + 2\dot{x} = D_y\Omega(x, y), \end{cases} \quad (27)$$

where

$$\Omega(x, y) = \frac{1}{2}(x^2 + y^2) + \frac{1 - \mu}{\sqrt{(x + \mu)^2 + y^2}} + \frac{\mu}{(x - 1 + \mu)^2 + y^2}.$$

The parameter μ stands for the relative mass of the two main bodies. For our tests we fixed $\mu = 0.0009537$ which corresponds to the Sun-Jupiter system.

The last ODE is the Galerkin projection of the following infinite dimensional ODE

$$\dot{a}_k = k^2(1 - \nu k^2)a_k - k \sum_{n=1}^{k-1} a_n a_{k-n} + 2k \sum_{n=1}^{\infty} a_n a_{n+k} \quad (28)$$

onto (a_1, \dots, a_{10}) variables. The above system describes solutions to the one-dimensional Kuramoto-Sivashinsky PDE [18, 34] under periodic and odd boundary conditions – see [45, 44] for derivation.

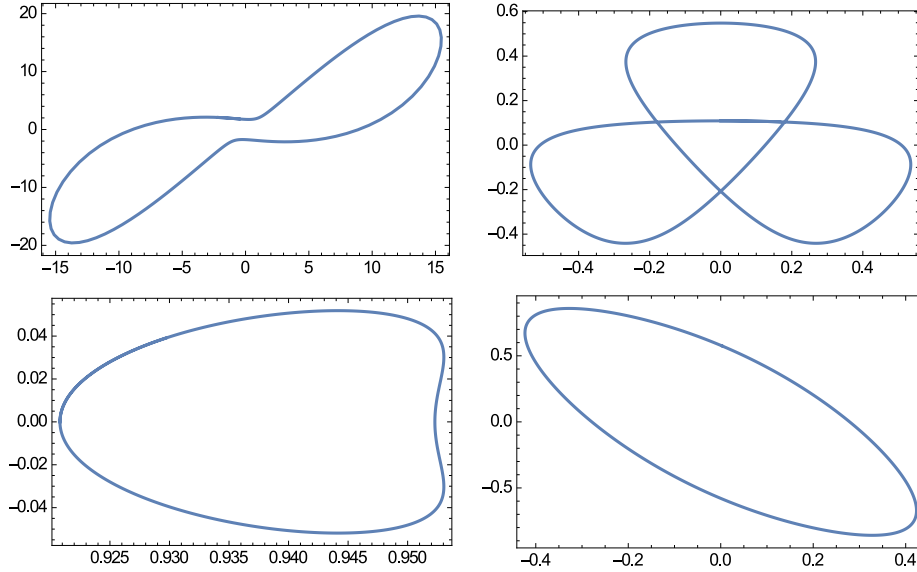


Figure 3: Approximate periodic orbits for (upper row) the Lorenz system (25), Hénon-Heiles hamiltonian (26), (lower row) the PCR3BP (27) and (28), respectively.

We have chosen initial conditions which are close to periodic orbits of these systems (see Fig. 3)

$$\begin{aligned}
 u_{\text{Lorenz}} &= (-2.1473681756955529387, 2.078047612582596404, 27), \\
 u_{\text{Hénon-Heiles}} &= (0.0, 0.10903, 0.5677233993382853, 0.0), \\
 u_{\text{PCR3BP}} &= (0.92080349132074, 0.0, 0.0, 0.1044476727069111), \\
 u_{\text{KS}} &= \begin{bmatrix} 0.2012106 \\ 1.2899797585174486 \\ 0.2012106 \\ -0.37786628185377774 \\ -0.042309451521292417 \\ 0.043161614695331821 \\ 0.0069402112803455653 \\ -0.0041564870501656455 \\ -0.00079448972725675504 \\ 0.00033160609117820303 \end{bmatrix}.
 \end{aligned}$$

For the two Hamiltonian systems the coordinates are given in the order (x, y, \dot{x}, \dot{y}) . The orbit u_{PCR3BP} is the well known L_1 Lyapunov orbit for the Sun-Jupiter-Oterma system. In [44] a computer assisted proof of the existence of a periodic solution for the full infinite dimensional system (28) is given. The projection of this periodic orbit onto first 10 coordinates is very close to the point u_{KS} . In fact, due to very strong dissipation the variables with high indexes have very small impact on the dynamics of (28). The system becomes very stiff even for relative small dimension of the Galerkin projection.

In Figs. 4–7 we present results of our numerical experiment. We can see that in each case the \mathcal{C}^1 -HO method does not return worse results than the \mathcal{C}^1 -Lohner

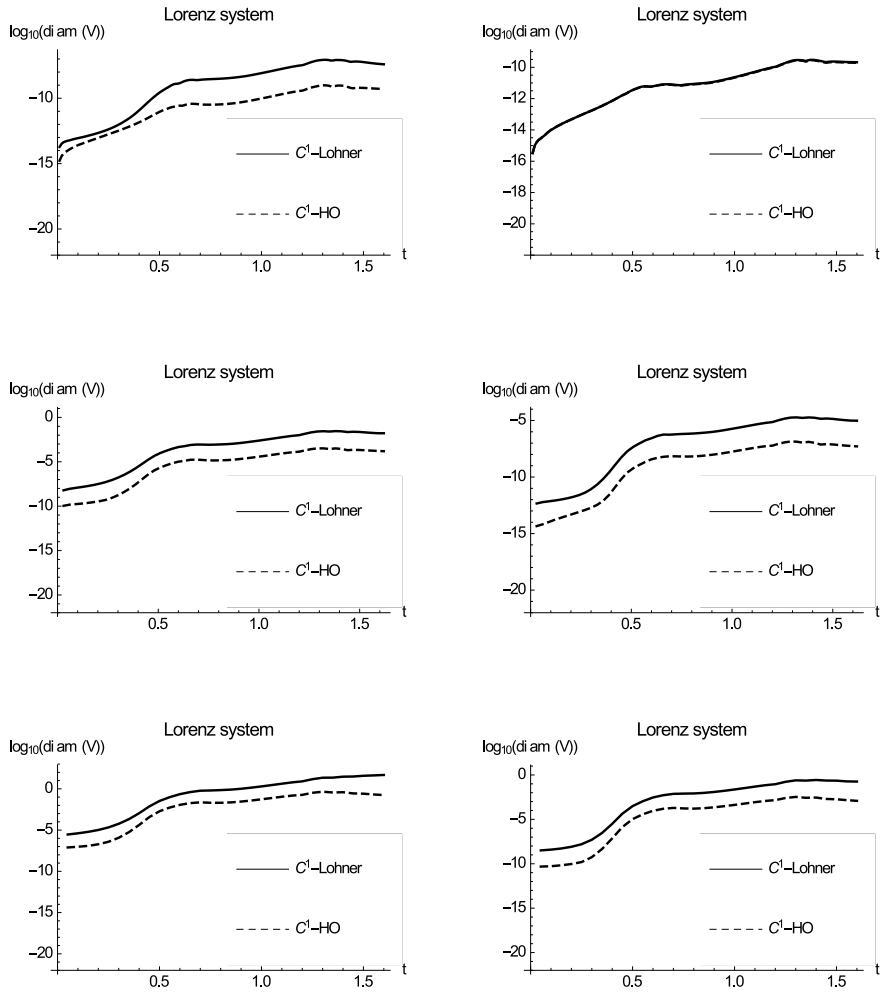


Figure 4: The results of the tests for the Lorenz system. Two columns correspond to orders $m = 10$ and $m = 15$, respectively. Rows correspond to fixed time steps $h \in \{0.01, 0.03, 0.05\}$, respectively.

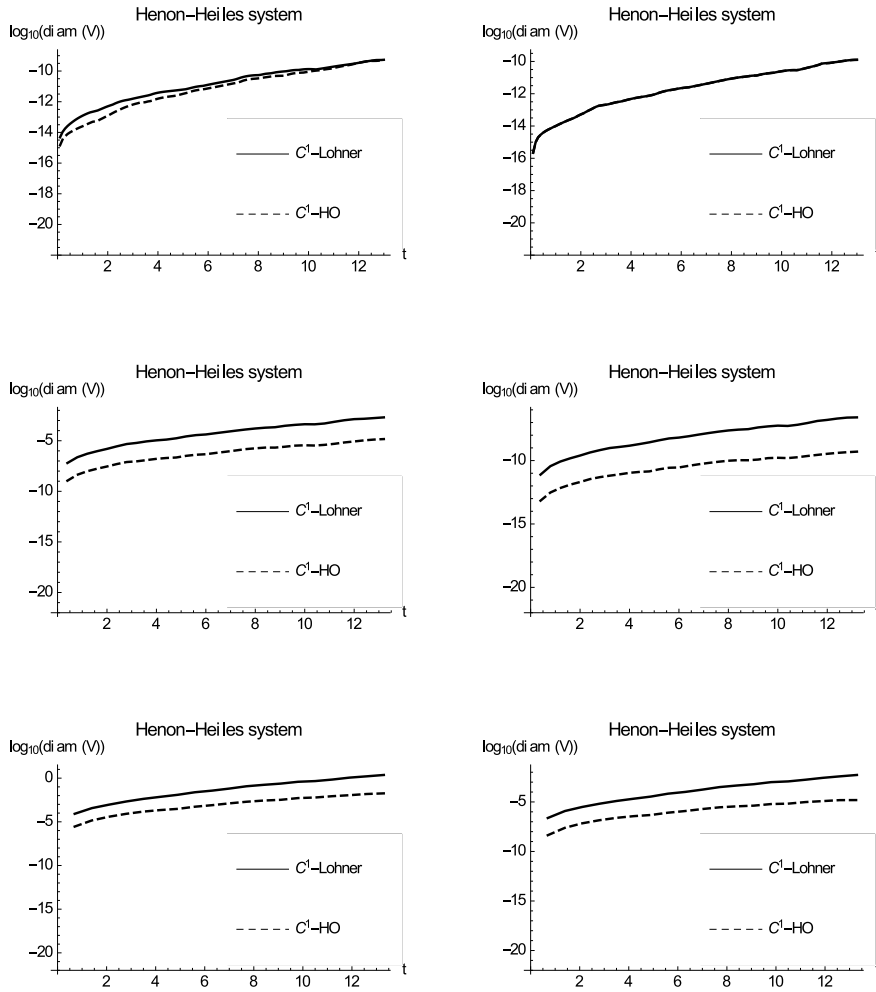


Figure 5: The results of the tests for the Hénon-Heiles system. Two columns correspond to orders $m = 10$ and $m = 15$, respectively. Rows correspond to fixed time steps $h \in \{0.1, 0.4, 0.7\}$, respectively.

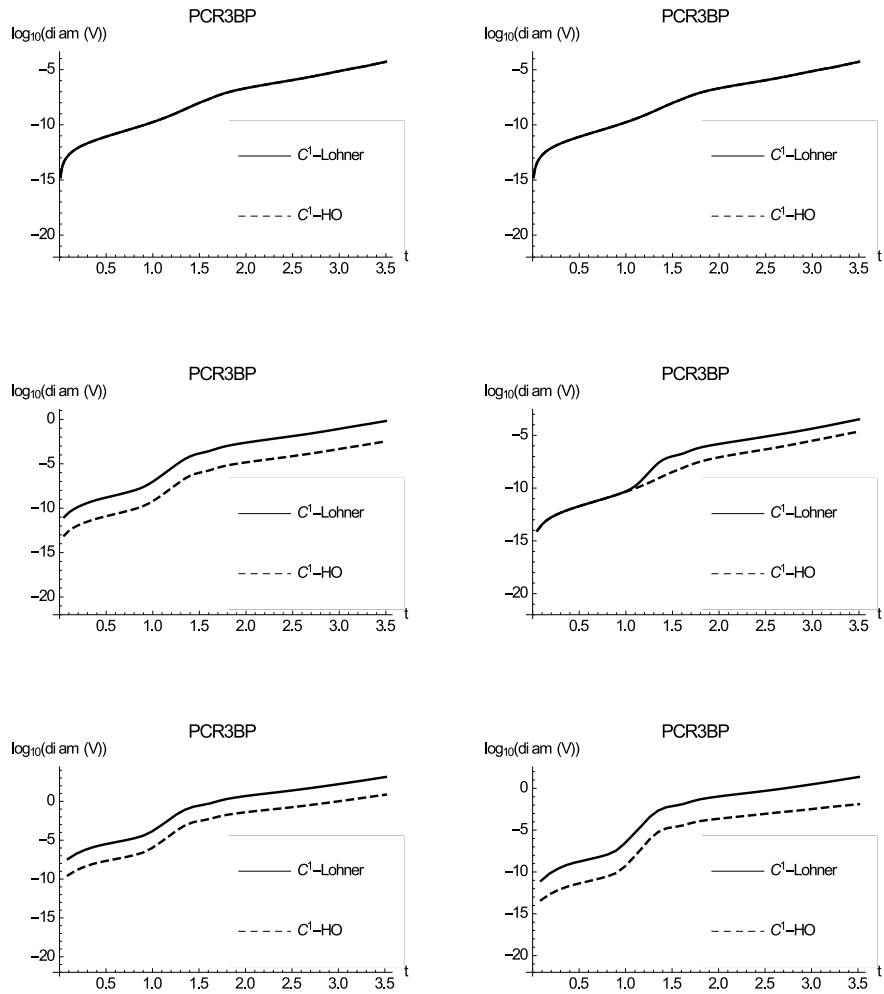


Figure 6: The results of the tests for the PCR3BP. Two columns correspond to orders $m = 10$ and $m = 15$, respectively. Rows correspond to fixed time steps $h \in \{0.01, 0.05, 0.09\}$, respectively.

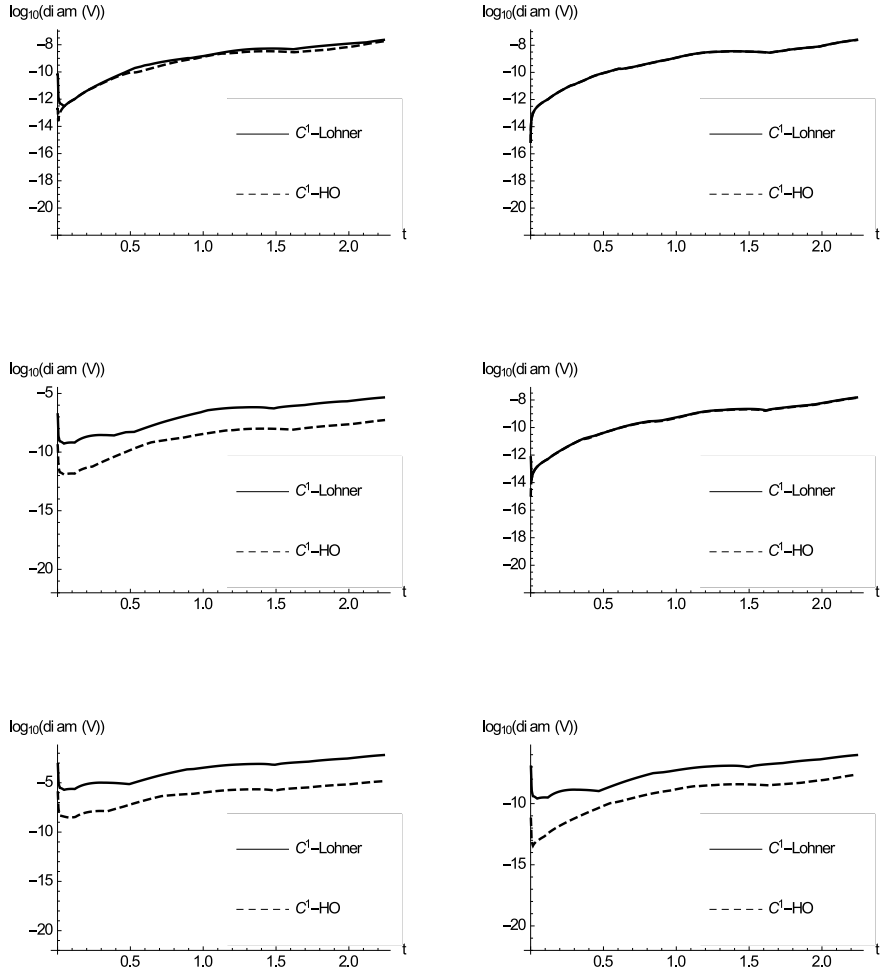


Figure 7: The results of the tests for the 10 dimensional Galerkin projection of the Kuramoto-Sivashinsky equation. Two columns correspond to orders $m = 10$ and $m = 15$, respectively. Rows correspond to fixed time steps $h \in \{0.0005, 0.001, 0.002\}$, respectively.

algorithm. This is due to its construction, because the bounds computed in the corrector step are intersected with the result from the predictor step which is used in the \mathcal{C}^1 -Lohner algorithm. Indeed, in the Algorithm 2 we have

$$[V] \leftarrow ([R] + [S][V^0]) \cap [V^0].$$

Looking at the columns of Figs. 4, 5 and 6 we observe that in each case, the advantage of the \mathcal{C}^1 -HO method increases when the time step is enlarged and the obtained bounds can be orders of magnitude tighter. This is due to the fact that the \mathcal{C}^1 -HO method has $c_q^{q,p}$ times tighter truncation error than the Taylor method. To give some numbers, let us take $m = 20$ which is a typical order used in computations. Then $p = q = 10$ and $c_q^{q,p} = c_{10}^{10,10} \approx 5.4 \cdot 10^{-6}$.

Increasing the order of method makes the truncation error of the \mathcal{C}^1 -Lohner method smaller when the time step is fixed. Therefore in the right columns of each figure we observe that the \mathcal{C}^1 -Lohner method performs much better than in the left column. The \mathcal{C}^1 -HO method, however, still returns tighter enclosures and is capable to make even larger time steps without significant lost of accuracy. This is especially important for stiff problems where the time steps cannot be large and thus integration over large time interval is very expensive. In Fig. 7 we can see that the \mathcal{C}^1 -HO method can perform much larger time steps keeping very good accuracy of computed bounds.

The bounds obtained by the \mathcal{C}^1 -HO method are tighter than those from the \mathcal{C}^1 -Lohner but as we observed in Section 3 the \mathcal{C}^1 -HO method is computationally more expensive. In the next section we will argue, that this extra cost per one step is compensated by the larger time steps we can make achieving the same error tolerance per one step specified by the user.

5 Applications.

In this section we present an application of the proposed algorithm to a computer assisted proof of a new result concerning the Rössler system [30]. We focus on the comparison of the time of computation needed to prove this result when the \mathcal{C}^1 -Lohner algorithm and the \mathcal{C}^1 -HO algorithm are used to integrate variational equations which is necessary to prove this theorem.

The classical Rössler system [30] is given by (2). When the two parameters a, b vary the system exhibits wide spectrum of bifurcations. The system admits period doubling bifurcations [40] which lead to chaotic dynamics [42]. In [27] the existence of two periodic orbits was proved by means of the Conley index theory. All the above results about the system (2) are computer assisted and use rigorous ODE solvers.

In this section we will give a new result concerning the system (2). The proof is computer assisted and it uses the proposed \mathcal{C}^1 -HO algorithm for rigorous integration of variational equation.

Let $\Pi = \{(x, y, z) \in \mathbb{R}^3 : x = 0 \text{ and } \dot{x} > 0\}$ be a Poincaré section – see Fig. 8 and let $P : \Pi \rightarrow \Pi$ be the Poincaré map. Since the x coordinate is equal to zero on Π we will use only two coordinates (y, z) to describe points on Π .

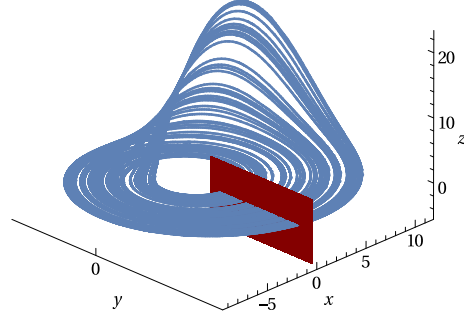


Figure 8: Typical chaotic trajectory of the system (2) and a slice of the Poincaré section Π .

Theorem 4 Put $l_B = -10.7$, $r_B = -2.3$, $l_M = 8.4$, $r_M = -7.6$, $l_N = -5.7$, $r_N = -4.6$, $Z = [0.028, 0.034]$ and

$$\begin{aligned} B &= [l_B, r_B] \times Z, \\ M &= [l_M, r_M] \times Z, \\ N &= [l_N, r_N] \times Z. \end{aligned}$$

For the classical parameter values $a = 0.2$, $b = 5.7$ the following statements hold true.

- The system (2) admits an attractor. The set B is a trapping region for the Poincaré map, i.e. P is well defined on B and $P(B) \subset B$. In particular, there exists a maximal invariant set $\mathcal{A} = \bigcup_{n>0} P^n(B)$ for the map P which is compact and connected.
- The maximal invariant set for P in $N \cup M$, denoted by $\mathcal{H} = \text{inv}(P, N \cup M) \subset \mathcal{A}$, is uniformly hyperbolic; in particular it is robust under perturbations of the system. The dynamics of P on \mathcal{H} is chaotic in the sense that $P|_{\mathcal{H}}$ is conjugated to the Bernoulli shift on two symbols.

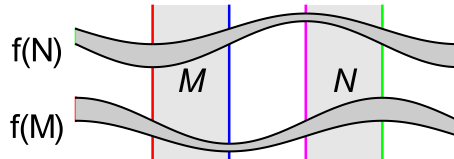


Figure 9: Geometric conditions that guarantee the existence of chaotic dynamics – see (29).

Proof: The tools used in a computer assisted proof of Theorem 4 are well known and we will shortly recall them.

Trapping region. Verification that B is a trapping region for P reduces to checking the inclusion

$$P(B) \subset B.$$

We uniformly subdivided the set B onto $N = 160$ pieces of the form $B_i = [a_i, a_{i+1}] \times Z$, $a_i = l_B + i * (r_B - l_B)/N$. Then we verified that $P(B_i) \subset B$. We used a rigorous ODE solver of order 25 from the CAPD library which implements the C^0 Hermite-Obreshkov algorithm proposed in [31].

Chaos. Semiconjugacy of $P|_{\mathcal{H}}$ to the Bernoulli shift is proved by means of the method of covering relations - the same as in [42] but applied to different sets. It is enough to check the following geometric conditions

$$\begin{aligned} \pi_y P^2(y, z) &< l_M && \text{for } (y, z) \in \{l_M\} \times Z, \\ \pi_y P^2(y, z) &> r_N && \text{for } (y, z) \in \{r_M\} \times Z, \\ \pi_y P^2(y, z) &< l_M && \text{for } (y, z) \in \{r_N\} \times Z, \\ \pi_y P^2(y, z) &> r_N && \text{for } (y, z) \in \{l_N\} \times Z, \end{aligned} \tag{29}$$

where π_y denotes canonical projection onto y coordinate. Geometry of these conditions is shown in Fig. 9. For the precise statement of a general theorem concerning the method of covering we refer to [42].

The conditions (29) have been verified in direct computation. We did not need to subdivide any of the four edges of N and M which appear in (29).

Hyperbolicity and full conjugacy. Uniform hyperbolicity of \mathcal{H} is proved by means of the cone condition introduced in [20]. Here we will use our algorithm for integration of variational equations which is necessary for rigorous computation of the derivative of Poincaré map P . Let Q be a diagonal matrix $Q = \text{Diag}(\lambda, \mu)$ with arbitrary coefficients satisfying $\lambda > 0$ and $\mu < 0$. It has been shown [38] that if for all $(y, z) \in N \cup M$ the matrix

$$DP^2(y, z)^T \cdot Q \cdot DP^2(y, z) - Q \tag{30}$$

is positive definite then the maximal invariant set in $N \cup M$ is uniformly hyperbolic. In our computations we used $\lambda = 1$ and $\mu = -100$.

We uniformly subdivided both sets N and M onto 48 and 32 equal pieces, respectively (only y coordinate was subdivided). Then, each rectangle has been submitted to our routine that integrates the first order variational equations and computes derivative of the Poincaré map P . Given a rigorous bound of the derivative we checked successfully the condition (30). Note that in the case of 2×2 matrix it is very easy to check positive definiteness of a matrix by the Sylvester criterion. ■

5.1 Comparison of time of computation.

In the section we will discuss how the CPU-time needed for verification of the uniform hyperbolicity in Theorem 4 depends on the choice of the algorithm used

to integrate variational equations. To this end, we did the following numerical experiment. For a fixed parameters

- m – the order of numerical method,
- tol – truncation error per one step of the numerical method,
- Alg – the algorithm used to integrate variational equations (\mathcal{C}^1 -Lohner or \mathcal{C}^1 -HO algorithm)

we compute the following three numbers

- $g_N(m, tol)$, $g_M(m, tol)$ - minimal natural numbers, such that using algorithm Alg , the method of order m with the tolerance tol we were able to check the cone condition (30) subdividing uniformly the sets N , M onto g_N and g_M , respectively,
- $t(Alg)$ – CPU time of checking the cone condition on both sets N and M with the algorithm and parameters as above.

m	tol	\mathcal{C}^1 -Lohner			\mathcal{C}^1 -HO			$\frac{t(Lo)}{t(HO)}$
		g_M	g_N	$t(Lo)$	g_M	g_N	$t(HO)$	
10	10^{-10}	39	33	0.90	48	32	0.82	1.10
10	10^{-12}	38	31	1.29	37	31	1.02	1.26
10	10^{-14}	25	31	1.69	23	30	1.20	1.41
10	10^{-16}	25	28	2.25	24	25	1.67	1.35
14	10^{-10}	45	52	1.13	48	48	0.84	1.34
14	10^{-12}	42	39	1.22	41	36	0.90	1.35
14	10^{-14}	47	33	1.65	49	33	1.21	1.36
14	10^{-16}	36	32	1.70	36	31	1.38	1.23
18	10^{-10}	63	77	1.67	62	56	1.20	1.40
18	10^{-12}	48	56	1.41	63	49	1.26	1.12
18	10^{-14}	44	43	1.76	47	38	1.18	1.50
18	10^{-16}	40	37	1.91	54	34	1.44	1.33
22	10^{-10}	151	95	3.36	101	67	1.93	1.74
22	10^{-12}	78	78	2.44	59	58	1.81	1.35
22	10^{-14}	52	61	2.05	61	49	1.56	1.32
22	10^{-16}	45	41	1.80	47	47	1.53	1.17

Table 1: Comparison of \mathcal{C}^1 -Lohner and \mathcal{C}^1 -HO algorithms.

Let us emphasize that the vector field of the Rössler system (2) contains only one nonlinear term. Hence we have $c_f = 1$ and this is almost the worst linear

case for the \mathcal{C}^1 -HO method when the complexity is dominated by the matrix operations – see analysis in Section 3.

In Table 1 we present results of this experiment. We see that in each case the \mathcal{C}^1 -HO algorithm is faster than the \mathcal{C}^1 -Lohner algorithm. Higher computational complexity of the \mathcal{C}^1 -HO algorithm is compensated by significantly smaller truncation error. Therefore a routine that predict the time step (the same routine was used in both cases) returns larger time steps for the \mathcal{C}^1 -HO algorithm and in consequence the total time of computation is smaller. We also notice that in some cases decreasing the tolerance increases the number of subdivisions g_N and g_M needed to check the cone condition – see for instance the row with $m = 14$ and $tol = 10^{-14}$. This is a consequence of many heuristics made in the implementation (for instance reorganization of doubleton representation after reaching some threshold values). These heuristics make the algorithm discontinuous with respect to parameters. Moreover, decreasing the tolerance increases number of time steps needed to compute full trajectory. This may result in weaker control of unavoidable wrapping effect.

6 Conclusions.

Since the \mathcal{C}^1 -Lohner algorithm appeared [43] it has been proved to be very useful in rigorous analysis of ODEs. In this paper we propose an efficient alternative for this algorithm and we provide free implementation of both \mathcal{C}^1 -Lohner and \mathcal{C}^1 -HO algorithms available as a module of the CAPD library [11]. Numerical tests show that the \mathcal{C}^1 -HO algorithm is slightly faster than the widely used \mathcal{C}^1 -Lohner algorithm. We have shown that the \mathcal{C}^1 -HO algorithm may be faster in practical applications. This is not very important when the total time of computation is counted in seconds, as we have seen in Section 5. Any progress matters, however, if a problem requires hundreds or thousands CPU hours: for example verification of the existence of an uniformly hyperbolic attractor of the Smale-Williams type [38] or the coexistence of chaos and hyperchaos in the 4D Rössler system [4]. In the computation reported in [4] the proposed \mathcal{C}^1 -HO algorithm has been used.

In [41] an algorithm for integration of higher order variational equations is presented. Ideas from Section 2 can be directly used to design and implement an algorithm, let us call it \mathcal{C}^r -HO, with the \mathcal{C}^r -Lohner method as a predictor step. This requires rather encoding than the theoretical effort and, we hope, this implementation will be available soon as a part of the CAPD library [11].

References

- [1] G. Alefeld, *Inclusion methods for systems of nonlinear equations - the interval Newton method and modifications*, in Topics in Validated Computations, J. Herzberger (Editor), Elsevier Science B.V., 1994, pages 7–26.

- [2] R. Barrio, M. Rodríguez, *Systematic Computer Assisted Proofs of periodic orbits of Hamiltonian systems*, Comm. Non. Sci. Num. Sim. 19 (8), 2660-2675.
- [3] R. Barrio, M. Rodríguez, F. Blesa, *Computer-assisted proof of skeletons of periodic orbits*, Comp. Phys. Commun. 183 (1), 80–85, (2012).
- [4] R. Barrio, M.A. Martínez, S. Serrano, D. Wilczak, *When chaos meets hyperchaos: 4D Rössler model*, Physics Letters A, Vol. 379, No. 38, 2300-2305 (2015).
- [5] M. Berz, K. Makino, *New Methods for High-Dimensional Verified Quadrature*, Reliable Computing, 5, 13-22 (1999).
- [6] M. Capiński, *Computer assisted existence proofs of Lyapunov orbits at L_2 and transversal intersections of invariant manifolds in the Jupiter-Sun PCR3BP*, SIAM J. Appl. Dyn. Syst. 11 (2012), no. 4, 1723-1753.
- [7] M. Capiński, A. Wasieczko-Zajac, *Geometric proof of strong stable/unstable manifolds with application to the restricted three body problem*, Top. Meth. Non. Anal. Vol. 46, No. 1, 2015, 363399.
- [8] K. Makino, M. Berz, *COSY INFINITY Version 9*, Nuclear Instruments and Methods A558 (2005) 346-350.
- [9] G.F. Corliss, R. Rihm, *Validating an a priori enclosure using high-order Taylor series*, In G. Alefeld and A. Frommer, editors, Scientific Computing, Computer Arithmetic, and Validated Numerics, pages 228–238. Akademie Verlag, Berlin, 1996.
- [10] K. Makino, M. Berz, *Rigorous Integration of Flows and ODEs using Taylor Models*, Symbolic Numeric Computation 2009, (2009) 79-84.
- [11] CAPD – Computer Assisted Proofs in Dynamics group, a C++ package for rigorous numerics, <http://capd.ii.uj.edu.pl>.
- [12] Z. Galias, *Counting low-period cycles for flows*, Int. J. Bifurcation and Chaos, Vol. 16, No. 10, 2873–2886 (2006).
- [13] Z. Galias, W. Tucker, *Rigorous study of short periodic orbits for the Lorenz system*, in: Proc. IEEE Int. Symposium on Circuits and Systems, ISCAS'08, Seattle, 764–767, (2008).
- [14] A. Griewank, *ODE solving via automatic differentiation and rational prediction*, in Numerical Analysis 1995 (Dundee, 1995), Pitman Res. Notes Math. Ser. 344, Longman, Harlow, UK, 1996, pp. 3656.
- [15] M. Hénon, C. Heiles, *The applicability of the third integral of motion*, Astron. J. 69 (1964), 449–457.

- [16] R. Krawczyk, Newton-Algorithmen zur Bestimmung von Nullstellen mit Fehlerschranken, *Computing* 4, 187-201 (1969).
- [17] T. Kapela, C. Simó, *Computer assisted proofs for non-symmetric planar choreographies and for stability of the Eight*, *Nonlinearity* 20 (2007) 1241-1255.
- [18] Y. Kuramoto, T. Tsuzuki, *Persistent propagation of concentration waves in dissipative media far from thermal equilibrium*, *Prog. Theor. Phys.*, 55,(1976), 365.
- [19] T. Kapela, P. Zgliczyński, *The existence of simple choreographies for the N-body problem - a computer assisted proof*, *Nonlinearity*, vol. 16, 1899-1918, (2003).
- [20] H. Kokubu, D. Wilczak and P. Zgliczyński, *Rigorous verification of cocoon bifurcations in the Michelson system*, *Nonlinearity*, **20** (2007), 2147–2174.
- [21] E. Lorenz, *Deterministic non-periodic flow*, *J. Atmos. Sci.* 20, 130–141 (1963).
- [22] R.J. Lohner, *Computation of Guaranteed Enclosures for the Solutions of Ordinary Initial and Boundary Value Problems*, in: *Computational Ordinary Differential Equations*, J.R. Cash, I. Gladwell Eds., Clarendon Press, Oxford, 1992.
- [23] R.E. Moore, *Interval Analysis*. Prentice Hall, Englewood Cliffs, N.J., 1966.
- [24] M. Mrozek, P. Zgliczyński, *Set arithmetic and the enclosing problem in dynamics*, *Annales Pol. Math.*, 2000, 237–259
- [25] A. Neumeier, *Interval methods for systems of equations*, Cambridge University Press, 1990.
- [26] N. Obreshkov, *Neue Quadraturformeln*, *Abh. Preuss. Akad. Wiss. Math. Nat. Kl.*, **4** (1940).
- [27] P. Pilarczyk, Topological numerical approach to the existence of periodic trajectories in ODE's, *Discrete and Continuous Dynamical Systems, A Supplement Volume: Dynamical Systems and Differential Equations*, 701-708 (2003)
- [28] L.B. Rall, *Automatic Differentiation: Techniques and Applications*, Vol. 120 of *Lecture Notes in Computer Science*. Springer Verlag, Berlin, 1981.

- [29] A. Rauh, M. Brill, C. Günther *A Novel Interval Arithmetic Approach for Solving Differential-Algebraic Equations with ValEncIA-IVP*, Special Issue of the International Journal of Applied Mathematics and Computer Science AMCS on Verified Methods: Applications in Medicine and Engineering, Vol. 19, No.3, pp. 381-397, 2009.
- [30] O.E. Rössler, An Equation for Continuous Chaos, *Physics Letters* Vol. 57A no 5, pp 397–398, 1976.
- [31] N.S. Nedialkov, K.R. Jackson, *An interval Hermite-Obreschkoff method for computing rigorous bounds on the solution of an initial value problem for an ordinary differential equation.* in *Developments in reliable computing (Budapest, 1998)*, 289–310, Kluwer Acad. Publ., Dordrecht, 1999.
- [32] N.S. Nedialkov, K.R. Jackson and G.F. Corliss, *Validated Solutions of Initial Value Problems for Ordinary Differential Equations*, Applied Mathematics and Computation, 105(1), 21-68, 1999.
- [33] N.S. Nedialkov, K.R. Jackson, John D. Pryce, *An Effective High-Order Interval Method for Validating Existence and Uniqueness of the Solution of an IVP for an ODE*, Reliable Computing, Volume 7, Issue 6, pp 449-465, 2001.
- [34] G.I. Sivashinsky, *Nonlinear analysis of hydrodynamical instability in laminar flames 1. Derivation of basic equations*, Acta Astron. 4 (1977), no. 11-12, 11771206.
- [35] R. Szczelina, P. Zgliczyński *A Homoclinic Orbit in a Planar Singular ODE - A Computer Assisted Proof*, SIAM J. Appl. Dyn. Syst., 12(3), 15411565 (2013).
- [36] W. Tucker, *A rigorous ODE solver and Smale's 14th problem*, Found. Comput. Math. Vol. 2, No. 1 (2002) 53–117.
- [37] N.S. Nedialkov, *VNODE-LP: A Validated Solver for Initial Value Problems in Ordinary Differential Equations*, Technical Report CAS-06-06-NN (2006).
- [38] D. Wilczak, *Uniformly hyperbolic attractor of the Smale-Williams type for a Poincaré map in the Kuznetsov system*, SIAM Journal on Applied Dynamical Systems, Vol. 9, No. 4, 1263–1283 (2010).
- [39] D. Wilczak and P. Zgliczyński, *Computer assisted proof of the existence of homoclinic tangency for the Hénon map and for the forced-damped pendulum*, SIAM J. Appl. Dyn. Syst. 8, Issue 4, pp. 1632–1663 (2009).
- [40] D. Wilczak and P. Zgliczyński. *Period doubling in the Rössler system - a computer assisted proof.* Found. Comp. Math. 9 (2009) 611–649.

- [41] D. Wilczak, P. Zgliczyński, *C^r -Lohner algorithm*, Schedae Informaticae, Vol. 20, 9-46 (2011).
- [42] P. Zgliczyński, *Computer assisted proof of chaos in the Hénon map and in the Rössler equations*, Nonlinearity, 1997, Vol. 10, No. 1, 243–252.
- [43] P. Zgliczyński, *C^1 -Lohner algorithm*, Foundations of Computational Mathematics, (2002) 2:429–465.
- [44] P. Zgliczyński, *Rigorous numerics for dissipative Partial Differential Equations II. Periodic orbit for the Kuramoto-Sivashinsky PDE - a computerassisted proof*, Found. Comp. Math., 4 (2004), 157–185.
- [45] P. Zgliczyński, K. Mischaikow, *Rigorous Numerics for Partial Differential Equations: the Kuramoto-Sivashinsky equation*, Found. Comp. Math. (2001) 1:255-288.